

# **Amyloidogenicity, Cytotoxicity and Receptor Activity of Bovine Amylin; Implications for Xenobiotic Transplantation and the Design of Non-toxic Amylin Variants**

Rehana Akter,<sup>1</sup> Rebekah L. Bower,<sup>2</sup> Andisheh Abedini,<sup>3</sup> Ann Marie Schmidt,<sup>3</sup> Debbie L. Hay<sup>2</sup> and Daniel P. Raleigh<sup>1, 4, \*</sup>

<sup>1</sup>Department of Chemistry, Stony Brook University, Stony Brook, NY 11794-3400.

<sup>2</sup>School of Biological Sciences and Maurice Wilkins Centre for Molecular Biodiscovery, University of Auckland, Auckland, 1142, New Zealand

<sup>3</sup>Diabetes Research Program, NYU School of Medicine, 522 First Avenue, New York, NY 10016.

<sup>4</sup>Graduate Program in Biochemistry and Structural Biology, Stony Brook University, Stony Brook, NY 11794.

\*Author to whom correspondence should be addressed, DPR; email, daniel.raleigh@stonybrook.edu; phone, (631) 632-9547; fax, (631) 632-7960.

**Running Title:** Amyloidogenicity of Bovine Amylin

**Keywords:** Amylin, Amyloid, Islet Amyloid Polypeptide, Amylin-Receptor, Diabetes,  $\beta$ -cell, Islet Transplantation.

## ABSTRACT

Islet amyloid formation contributes to  $\beta$ -cell death and dysfunction in type-2 diabetes and to the failure of islet transplants. Amylin (Islet amyloid polypeptide, IAPP), a normally soluble 37 residue polypeptide hormone produced in the pancreatic  $\beta$ -cells, is responsible for amyloid formation in type-2 diabetes. The peptide is deficient in type-1 diabetes. Amylin normally plays an adaptive role in metabolism and the development of non-toxic, non-amyloidogenic, bioactive variants of human amylin are of interest for use as adjuncts to insulin therapy. Naturally occurring non-amyloidogenic variants are of interest for xenobiotic transplantation and because they can provide clues towards understanding the amyloidogenicity of human amylin. The sequence of amylin is well conserved among species, but sequence differences strongly correlate with *in vitro* amyloidogenicity and with islet amyloid formation *in vivo*. Bovine amylin differs from the human peptide at ten positions and is one of the most divergent among known amylin sequences. We show that bovine amylin is not toxic to cultured  $\beta$ -cells and is considerably less amyloidogenic than the human polypeptide, but is only a low potency agonist at human amylin-responsive receptors. The bovine sequence contains several non-conservative substitutions relative to human amylin including His to Pro, Ser to Pro and Asn to Lys replacements. The effect of these substitutions is analyzed in the context of wild type human amylin; the results provide insight into their role in receptor activation, the mode of assembly of human amylin and into the design of soluble amylin analogs.

$\beta$ -cell death and dysfunction play central roles in the progression of type-2 diabetes. Pancreatic islet amyloid formation by the polypeptide hormone amylin (islet amyloid polypeptide, IAPP) is an important contributing factor.<sup>1, 2</sup> The deposition of islet amyloid also contributes to the failure of islet transplants and is one of the factors that limit the potential of this therapeutic approach for the treatment of type-1 diabetes.<sup>3, 4</sup> Human amylin (h-amylin) is a 37 residue polypeptide hormone that, in its soluble form, plays an adaptive role in metabolism, but aggregates to form pancreatic islet amyloid during the progression of type-2 diabetes.<sup>5-7</sup> The polypeptide is synthesized in the pancreatic  $\beta$ -cells, stored together with insulin in the insulin secretory granule and released in response to the same stimuli that leads to insulin secretion. h-Amylin, like insulin, is deficient in type-1 diabetes. Non-amyloidogenic variants of h-amylin have been developed for clinical use and one designed analog, Pramlintide (Symlin), has been approved by the FDA.<sup>8, 9</sup> Amylin causes meal-ending satiation and has also been under consideration for treating obesity. Thus, there is significant interest in understanding amylin behavior.

Not all organisms develop islet amyloid *in vivo* and the ability to do so correlates with *in vitro* amyloidogenicity and with the primary sequence of amylin.<sup>10</sup> Amylin has been found in all mammals examined and is well conserved, although there are variations. The peptide contains a conserved disulfide bridge between Cys-2 and Cys-7 and a conserved amidated C-terminus (Figure 1). The analysis of inter-species variations in amyloidogenicity can provide clues to the factors that influence the tendency of h-amylin to form amyloid and insight into the mechanism of h-amylin amyloid formation. Analysis of the amyloidogenicity and cytotoxicity of non-human amylin is also of interest from the perspective of xenobiotic transplantation. Along these lines, porcine islet grafts lead to improved long term glycemic control in laboratory animals while transplantation with human islet grafts results in only temporary improvement. Porcine amylin is

much less amyloidogenic than human amylin and this correlates with the improved glycemic control offered by porcine islet transplantation.<sup>4</sup> Non-amyloidogenic variants of h-amylin are also of interest as potential next generation adjuncts to insulin therapy.

The primary sequence of amylin is highly conserved, but not all species form amyloid *in vivo* and the ability to do so depends on the primary sequence.<sup>10</sup> Rat/mouse amylin (r-amylin) differs from the human peptide at six positions and five of these are located between residues 20 to 29 (Figure S1). Important early work focused on the role of the primary sequence in this region in determining amyloidogenicity.<sup>11</sup> More recent studies have shown that substitutions outside of the 20 to 29 segment can have significant effects on amyloid formation.<sup>12-14</sup> r-Amylin contains three proline residues in the 20-29 region, and this is believed to be an important factor contributing to the non-amyloidogenicity of r-amylin. r-Amylin also contains an H18R replacement and substitution of His with Arg has been shown to slow amyloid formation by h-amylin. h-Amylin and bovine amylin (b-amylin) differ at ten positions, four of which are located between residues 20 and 29. These include N22K, F23L, L27F and S29P replacements. N22K and S29P are the least conservative of these and are expected to reduce amyloidogenicity; N22K because it increases the net charge and S29P because Pro residues disrupt  $\beta$ -sheets. A F23L replacement in h-amylin has been shown to slow amyloid formation by a factor of 2 *in vitro*.<sup>15</sup> b-Amylin has several additional charged and proline residues outside of the 20 to 29 region relative to h-amylin (Figure 1). These include non-conservative H18P and N31K replacements as well as an A8E substitution. Overall, b-amylin contains 2 Pro residues and 5 charged residues at neutral pH, while h-amylin contains no Pro residues and 2 or 3 charged residues depending upon the protonation state of His-18.

Although b-amylin is one of the most divergent amylin sequences reported its ability to form amyloid, its potential toxicity towards  $\beta$ -cells and its activity toward human amylin receptors

have not been studied (Figure 1, Figure S1). Reports of diabetes in cattle are rare and have often been linked to bovine viral diarrhea (BVD) and it is not known if cows develop islet amyloid *in vivo* or if bovine amylin is amyloidogenic *in vitro*.<sup>16-18</sup> Here we examine the amyloidogenicity and cytotoxicity of b-amylin and the activity of b-amylin towards two amylin-responsive receptors, the h-amylin 1 subtype of receptor (AMY<sub>1</sub>) and the human calcitonin receptor. We specifically used the CT<sub>(a)</sub> form of the calcitonin receptor in the absence or presence of receptor activity-modifying protein (RAMP) 1.

## RESULTS

### **Bovine amylin is significantly less amyloidogenic than human amylin.**

We analyzed the h-amylin and b-amylin sequences using several standard amyloid prediction programs.<sup>19</sup> These programs employ different methodologies, but we found that all of them agree that b-amylin is less amyloidogenic than h-amylin (Table S1). However, it is important to experimentally evaluate the amyloidogenicity of b-amylin since amyloid prediction programs have been shown to give inconsistent results for other variants of amylin.<sup>20</sup>

Amyloid formation typically consists of a lag phase in which pre-amyloid species are formed, followed by a growth phase, during which fibrils elongate, and a final plateau phase in which fibrils are in equilibrium with the soluble peptides. We investigated the amyloidogenicity of b-amylin by using thioflavin-T binding fluorescence assays to measure the kinetics of amyloid formation and transmission electron microscopy (TEM) to test for the presence or absence of amyloid fibrils. Thioflavin is a small extrinsic fluorescence dye whose quantum yield increases when bound to amyloid fibrils.<sup>21</sup> The dye provides a convenient assay of amyloid formation

kinetics, but can lead to false negatives.<sup>20, 22, 23</sup> Consequently, we used TEM to independently monitor amyloid formation.

First, we studied the ability of b-amylin to form amyloid at pH 7.4 using 20 mM Tris buffer since Tris buffer has been extensively used in biophysical studies of amyloid formation by h-amylin. A typical sigmoidal thioflavin-T fluorescence kinetic curve was observed for h-amylin amyloid formation with a time to reach 50 % of the final fluorescence change,  $T_{50}$ , of 16 hours. TEM images revealed dense mats of amyloid fibrils (Figure 2). In contrast, no increase in thioflavin-T fluorescence signal was observed for b-amylin even after 6 days of incubation (Figure 2). TEM images were collected at different time points, and no amyloid fibrils were detected for the b-amylin samples even after 21 days of incubation (Figure 2).

We also compared amyloid formation by h-amylin and b-amylin in phosphate buffered saline (PBS, 10 mM phosphate 140 mM KCl) at pH 7.4. h-Amylin amyloid formation is very sensitive to added salt, the choice of the anion and is faster in PBS relative to Tris.<sup>24</sup> As expected, h-amylin amyloid formation was accelerated in PBS buffer and the  $T_{50}$  decreased to 3 hours (Figure S2). In contrast, no significant increase in thioflavin-T fluorescence signal was observed for b-amylin under these conditions, even after 7 days of incubation, and no amyloid fibrils were detected in TEM images of the b-amylin sample (Figure S2). In summary, we found that b-amylin is considerably less amyloidogenic than h-amylin under all conditions tested.

### **Bovine amylin is significantly less toxic towards cultured $\beta$ -cells**

We studied the effect of bovine amylin on  $\beta$ -cell viability using rat INS-1  $\beta$ -cells and using Alamar blue reduction assays. INS-1  $\beta$  cells are a pancreatic cell line that is widely used for amylin amyloid toxicity studies. We tested the effects on the  $\beta$ -cell viability of 15  $\mu$ M, 22  $\mu$ M and 30  $\mu$ M

b-amylin after 24 h, 48 h, and 84 h of incubation. h-Amylin was used as a positive control. 30  $\mu$ M h-amylin considerably decreased cell viability to 52 % after 24 h while b-amylin did not exhibit any toxicity (Figure 3). A further decrease in cell viability was induced by h-amylin after longer incubation times; cell viability declined to 38 % and 31 % at 48 h and 84 h respectively (Figure S3). In striking contrast, 30  $\mu$ M b-amylin was not toxic, even after 84 h incubation (Figure S3).

### **Bovine amylin weakly activates hCT<sub>(a)</sub> and hAMY<sub>1(a)</sub>**

In consideration of the potential value of bovine islet xenografts, it was of interest to determine the bioactivity of bovine amylin at human amylin receptors. Therefore, the biological activity of b-amylin and h-amylin were measured by analyzing the production of cAMP at the hCT<sub>(a)</sub> and hAMY<sub>1(a)</sub> receptors *in vitro*; this is a standard assay for amylin receptor activity.<sup>25</sup> Stimulation of cAMP production occurred with b-amylin at both receptors, however b-amylin was at least 300-fold less potent than h-amylin (Figure 4). Interestingly, b-amylin remained a partial agonist at the hCT<sub>(a)</sub> receptor, only reaching 40% of the E<sub>max</sub> compared to h-amylin while at the hAMY<sub>1(a)</sub> receptor, it was a full agonist. This is likely to be because we could not use sufficiently high peptide concentrations to achieve a full curve at the calcitonin receptor. A summary of the quantified data is presented in table 1.

### **Mutational analysis of human amylin provided insight into the reduced amyloidogenicity of bovine amylin**

We investigated several point mutants of h-amylin in order to probe the cause of the reduced amyloidogenicity of b-amylin. We tested single point variants of h-amylin corresponding to the four least conservative b-amylin substitutions H18P, N22K, S29P, N31K using thioflavin-

T assays and TEM. The Asn to Lys substitutions are unusual replacements in amylin and are expected to reduce amyloidogenic by increasing the net charge on the polypeptide. The consequences of Asn to Lys substitutions on h-amylin formation have not yet been reported. The proline residues at positions 18 and 29 in b-amylin are also of interest in a biophysical context. Pro is a well-known disrupter of secondary structure and is not compatible with the classic parallel, in register  $\beta$ -sheet structures which form the core of amyloid fibrils. Pro 18 is located in a region thought to be important for initial oligomerization during amylin aggregation and a proline at position 18 is a very unusual replacement (Figure S1). The Ser to Pro replacement at position 29 is not found in primates; h-amylin and amylin from other primates all have a serine at position 29. According to structural models of the h-amylin amyloid fibril, serine 29 forms key interactions with adjacent residues in the amyloid fibril core and these are presumably important for fibril structure and stability (Figure 1).<sup>26, 27</sup> Thus, a Ser to Pro substitution at position 29 should reduce amyloidogenicity. The S29P replacement is also one of the substitutions found in non-amyloidogenic r-amylin.

All the mutants reduced the rate of amyloid formation, but fibrils were still observed by TEM (Figure 5). H18P h-amylin had the greatest effect, lengthening  $T_{50}$  almost 4-fold to about 62 h in 20 mM Tris-HCl buffer (Figure S4). The  $T_{50}$  for N22K h-amylin, S29P h-amylin and N31K h-amylin were about 50 h, 29 h and 32 h respectively, representing approximately 3 to 2-fold increases in  $T_{50}$  under the conditions of these experiments (Figure S4). According to structural models of h-amylin, residues 18 and 22 are in a turn region of the amyloid fibril while residues 29 and 31 are in the C-terminal  $\beta$ -sheet structure and make key interactions with adjacent residues in the core of the amyloid fibril (Figure 1).<sup>26, 27</sup> Prior work has examined Asn to Leu replacements in a truncated variant of IAPP corresponding to residues 8 to 37. In that study, a N22L substitution

had very little effect on the rate of amyloid formation while an N31L mutation lead to approximately a 2-fold increase in  $T_{50}$ .<sup>14</sup> Our mutational analysis indicates that residues in the turn region have more effect on amyloidogenicity than at least some of the sites in the putative C-terminal  $\beta$ -strand of the amyloid fibril.

### **Mutational analysis of human amylin aids in understanding reduced $\beta$ -cell toxicity of bovine amylin**

We studied the effect of H18P, N22K, and S29P mutants on rat INS-1  $\beta$ -cells toxicity. Cell viability was measured using 30  $\mu$ M of each peptide after 24 h and 48 h incubation (Figure 6). The H18P mutant was the least toxic of the three variants. After 24 h of incubation, cell viability decreased only by 17 % and after 48 h by about 30 %. In contrast, h-amylin decreased cell viability by 48 % after 24h and by 62 % after 48 h incubation. 24 h incubation with the N22K variant reduced cell viability by 60 % and after 48 h incubation by about 73 %. Similarly, for the S29P variant, cell viability was decreased by 65 % and 71 % after 24 h and 48 h incubation respectively. Analysis of the toxicity profiles indicates that proline at position 18 has the most substantial effect on reduction of b-amylin toxicity.

### **Mutational analysis of human amylin to understand the decreased potency of bovine amylin at hAMY<sub>1(a)</sub> and hCT<sub>(a)</sub> receptors**

To understand the drastic potency reduction of the b-amylin peptide at hCT<sub>(a)</sub> and hAMY<sub>1(a)</sub> receptors, the same four h-amylin peptides with single point mutations from the bovine sequence were analyzed for their activity at amylin-responsive receptors (Table 1 and Figure 7). The peptide substitution with the largest impact on potency was H18P, resulting in potency reductions of 7 and

20-fold at the hCT<sub>(a)</sub> and hAMY<sub>1(a)</sub> receptors, respectively. Despite the reductions in potency, this analog remained a full agonist at both receptors. The S29P, N22K and N31K substitutions were well tolerated, with no detrimental impact on receptor activity at either receptor. The data are summarized in table 1.

The results presented here clearly show that b-amylin is considerably less amyloidogenic than h-amylin, less toxic to  $\beta$ -cells and is weakly potent at h-amylin and calcitonin receptors. The considerable reduction in activity towards h- amylin responsive receptors indicates that bovine islets are not suitable candidates for xenobiotic transplantation.

The mutational analysis indicates that the His 18 to Pro substitution plays a major role in the reduced amyloidogenicity, reduced toxicity and reduced receptor activity of b-amylin. Analysis of the H18P mutant provides insight into amyloid formation by wild type h-amylin amyloid formation. One model of h-amylin amyloid formation posits that the process is initially driven by association of transiently populated helical conformers of amylin where the helical structure is localized in the N-terminal half to two-thirds of the molecule. This in turn generates a high local concentration of the C-terminal region of the peptide which promotes the formation of the cross  $\beta$ -sheet structure.<sup>28</sup> Residue 18 is in a region proposed to be important for the initial helical oligomerization<sup>28-31</sup> and proline is energetically very unfavorable in a  $\alpha$ -helix. The reduced rate of amyloid formation is consistent with this region playing a role in aggregation despite the fact that it falls outside of the putative amyloidogenic core of h-amylin. However, the H18P mutant does form amyloid, arguing that helical structure at or adjacent to His-18 is not a strict requirement for h-amylin amyloid formation. The transition from oligomers to  $\beta$ -sheet rich amyloid fibrils has been proposed to occur through the transient formation of parallel, in register, intermolecular,  $\beta$ -sheet structure localized near Phe-23 within the 20-29 region of hIAPP. This structure develops

during the lag phase and serves to align the peptide strands in register; the structure is then disrupted during the transition to the final fibril state and the development of cross- $\beta$  structure in other regions of the molecule. This model predicts that substitutions within the turn region should influence the kinetics of amyloid fibril formation even if the substitutions are at sites which are not part of the cross- $\beta$  core of the fibril. The exact extent, in terms of participating residues, of the transient  $\beta$ -sheet are not yet known, but the sensitivity of the kinetics of amyloid formation to substitutions at residue 22 is consistent with this model.

The analysis of the N22K and N31K variants shows that charged residues as well as proline substitutions make important contributions to reducing amyloidogenicity, consistent with earlier studies that examined H18R and S20K variants of h-amylin.<sup>32, 33</sup> That work together with the present study indicates the substitution with charged residues at key locations is a straight forward strategy for reducing amyloidogenicity.

It is interesting that despite being 73% identical with h-amylin, b-amylin had such a substantial reduction in receptor potency. This is likely due to the fact that we used human rather than bovine receptors. There is little information about amylin activity across species, although h-amylin is reported to be active at porcine calcitonin and amylin receptors.<sup>34</sup> It is not known if porcine amylin is active at human receptors. Rat amylin and h-amylin have similar potency at their respective receptors<sup>35</sup> and r-amylin is 78% identical to b-amylin. It is evident from the functional data that the proline at position 18 in place of the native histidine contributes towards the reduced potency. Adding a proline at this position may have interfered with important side-chain interactions made by basic histidine side chain of h-amylin or may have unfavorably altered the secondary structure of the peptide, as proline is well-known to be secondary structure-disrupting. Amylin receptors are composed of the calcitonin receptor in complex with a receptor activity

modifying protein (RAMP). There are no structures of amylin bound to an amylin responsive receptor.<sup>36, 37</sup> Amylin is a member of the CGRP family of polypeptide hormones and these molecules are proposed to contain an amphiphilic helix located in the first 1/2 to 2/3 of the molecule that starts after the disulfide, and which may be important for receptor binding. Structures of fragments of CGRP, adrenomedullin and calcitonin bound to the extracellular domain of these receptors show that the C terminal portion of the peptides in this family contain a turn, but do not bind to this part of the receptor in a helical conformation. Models of the C-terminal portion of amylin bound to amylin receptors suggests that amylin binds in a similar manner<sup>38, 39</sup> and it is likely that the peptide helix binds to the extracellular loops or transmembrane bundle of the receptor. A Pro at position 18 is likely to significantly destabilize ordered structure in this region of the peptide, potentially rationalizing the significant effect of the H18P substitution. Interestingly, in every other species of amylin, the residue at position 18 is a strongly conserved basic arginine or histidine only deviating in the bovine sequence (Figure S1). Conversely, a proline substitution at position 29 in place of the native serine found in h-amylin had no significant effect on peptide potency. This residue is a proline apart from humans, monkeys, macaques, and baboons which possess a serine, suggesting that prolines are relatively well conserved here and do not impose unfavorable structure disruptions at the peptide-receptor interface. This was perhaps expected as both rat amylin and pramlintide also possess a proline at position 29 and are either equipotent<sup>35</sup> or more potent<sup>9</sup> than h-amylin at human amylin receptors, respectively.

Two other well-tolerated substitutions were the lysine for asparagine replacements at positions 22 and 31. Prior work has shown that *in vitro* glycosylation of h-amylin at position N22 or N31 did not eliminate *in vitro* receptor activity.<sup>40</sup> Taken together, that work and the present study reveals that h-amylin is remarkably tolerant to substitution at these sites; neither increased

bulk induced by glycosylation, nor substitution of a charged residue has a major impact. Thus, these sites are strong candidates for modification to develop less amyloidogenic, but active variants of h-amylin. Replacing asparagine residues should have the added benefit of reducing potential susceptibility to deamidation.<sup>41-43</sup>

The data presented here show that the bovine polypeptide, while considerably less toxic and considerably less amyloidogenic than the human hormone, is not a suitable candidate for therapeutic use given its low potency towards human amylin receptors. The non-conservative H18P replacement makes a major contribution to the reduced potency; highlighting the importance of this region for polypeptide- receptor interactions. In contrast, the minimal effect on activity deduced for the N22K, S29P and N31K replacements, together with earlier studies on r-amylin, highlights the tolerance of h-amylin to substitutions in the C-terminal half of the molecule. Thus, targeting residues in this region of the polypeptide is likely to be a fruitful approach for designing amylin variants with lower propensity to aggregate and increased solubility, but which retain biological activity. Of particular interest in this regard is the potential for replacing Asn-22 and /or Asn-31 with charged residues. Asn substitutions have not yet been incorporated in reported soluble analogs of h-amylin.<sup>8, 44</sup>

## **MATERIALS AND METHODS**

**Peptide Synthesis and Purification:** Standard Fmoc (9-fluorenylmethoxy carbonyl) solid phase peptide synthesis methods were used to prepare h-amylin, b-amylin, H18P h-amylin, N22K h-amylin, S29P h-amylin and N31K h-amylin. Peptides were synthesized on a 0.1 mmol scale using a CEM Liberty automated microwave peptide synthesizer. Fmoc-PAL-PEG-PS resin (Applied Biosystems) was used to obtain an amidated C-terminus. Fmoc protected pseudoproline

(Oxazolidine) dipeptide derivatives were used to facilitate the synthesis and employed as described. HBTU (O-(Benzotriazol-1-yl)-N, N, N', N'- tetramethyluronium hexafluorophosphate) was used as a coupling agent. The first amino acid attached to the resin, pseudoproline dipeptide derivatives, and all  $\beta$ -branched amino acids were double coupled. All solvents were ACS grade. Fmoc protected amino acids and all other reagents were purchased from AAPPTec, Novabiochem, Sigma-Aldrich, VWR and Fisher Scientific. Standard trifluoroacetic acid (TFA) cleavage conditions were used to cleave the peptide from the resin and to remove the side chain protecting groups. Crude peptides were precipitated with cold diethyl ether. Crude peptides were dissolved in 20% acetic acid (v/v) and freeze dried to increase the solubility of the peptide and were then dissolved in 100% DMSO (Dimethyl sulfoxide) to promote intramolecular disulfide bond formation. Disulfide bond formation was confirmed by matrix-assisted laser desorption ionization time of flight mass spectrometry (MALDI-TOF MS). The oxidized peptides were purified via reversed-phase HPLC using a C18 preparative column. A two-buffer solution system was used. Buffer A was 100% H<sub>2</sub>O and 0.045% HCl and buffer B was 80% ACN (Acetonitrile), 20% H<sub>2</sub>O and 0.045% HCl. A gradient of 20% to 60% buffer B in 40 min was used. HCl was used as an ion pairing agent instead of TFA because TFA can influence amylin aggregation kinetics and can also affect amylin cell toxicity studies. The freeze-dried peptides were dissolved in HFIP (1, 1, 1, 3, 3, 3-Hexafluoro-2-propanol) after the first purification to remove residual scavengers and re-purified via reverse-phase HPLC. The purity of the peptides was confirmed by reversed-phase HPLC using a C18 analytical column. The molecular weight of the purified oxidized peptides were confirmed by MALDI-TOF MS: h-amylin expected, 3903.3; observed 3903.3; bovine amylin, expected, 3906.5; observed, 3906.6; H18P h-amylin, expected 3866.3; observed, 3866.4; S29P h-amylin

expected, 3913.4; observed, 3913.0; N22K h-amylin, expected 3917.4; observed 3917.6; N31K h-amylin expected 3917.4; observed 3917.3.

**Fluorescence Assays:** A 0.5 mM peptide stock solution in 100% HFIP was prepared from the dry peptide. Aliquots were filtered through a 0.22  $\mu\text{m}$  Millex syringe-driven membrane filter. The concentration of the stock solution was determined by measuring the UV absorbance at 280 nm. Desired amounts of peptide stock solution were aliquoted and freeze dried to remove HFIP.

Thioflavin-T binding fluorescence assays were conducted using a Beckman Coulter DTX 880 Multimode Detector plate reader and a Spectramax Gemini EM plate reader. Corning 96-well non-binding surface black plates with lids were used and were sealed with polyethylene sealing tape. Thioflavin-T fluorescence was measured with 450 nm excitation and the emission at 485 nm was monitored. 20 mM Tris-HCl buffer and thioflavin-T solution were added to freeze dried peptide right before the assay and thioflavin-T fluorescence was measured immediately. Experiments with 10 mM phosphate buffer and with 140 mM salt were performed in an identical fashion. All the experiments used: 16  $\mu\text{M}$  amylin, 32  $\mu\text{M}$  thioflavin-T, 25°C, pH 7.4 and no agitation.

**Transmission Electron Microscopy:** TEM images were recorded using an FEI Bio TwinG<sup>2</sup> Transmission Electron Microscope at the central microscopy center at Stony Brook University. 18  $\mu\text{L}$  of peptide solution was taken at the end of the kinetic runs. Samples were blotted on a carbon-coated formvar 300-mesh copper grid for 1 min and then negatively stained with 2% uranyl acetate for 1 min. Images were taken at a 68,000X magnification and 100 nm under focus.

**Cytotoxicity Assays:** Rat INS-1  $\beta$ -cells were seeded at a density of 40,000 cells per well in 96-well plates 24 hours prior to the start of experiments.<sup>45</sup> Peptides were dissolved in complete RPMI, and incubated on cells for 24, 48 and 84 hours prior to cell viability measurements.  $\beta$ -cell viability was assessed using AlamarBlue assays. AlamarBlue was diluted ten-fold in culture media and incubated on cells for 5 hours at 37°C. Fluorescence (excitation 530 nm; emission 590 nm) was measured with a Beckman Coulter DTX880 plate reader. Values were calculated relative to untreated control cells.

**Cell culture and transient transfections:** Cos-7 cells were cultured and transfected for receptor activity assays as previously described<sup>46</sup>. In brief, cells were cultured in Dulbecco's modified eagle medium (DMEM) with 8% heat-inactivated fetal bovine serum (FBS) and kept in a 37°C humidified 95% air/5% CO<sub>2</sub> incubator. Cells were plated at a density of 18,000 – 20,000 cells/well (depending on cell passage) in 96-well culture plate and returned to the incubator for approximately 18-24 hours. Transient transfections were carried out using polyethyleneimine (PEI) as described previously<sup>46</sup> and maintained at 37°C in a humidified 95% air/5% CO<sub>2</sub> incubator for 36 – 48 hours. All DNA constructs used in these experiments were in pcDNA3.1 vectors. The insert-negative human CTR with leucine at the polymorphic amino acid position 447 with an N-terminal haemagglutinin (HA) tag (HA-hCTR) and myc-tagged hRAMP1 were utilized in these experiments.

**cAMP Assays:** Measurement of intracellular cAMP was achieved using a time-resolved fluorescent resonance energy transfer assay (LANCE cAMP assay, PerkinElmer), similar to the previously described Alphascreen assay,<sup>47</sup> with the following changes. Following stimulation with

peptide agonist, cAMP assay media from the wells was thoroughly aspirated and 50  $\mu$ l of ice-cold absolute ethanol added to each well. Plates were then placed in a  $-30^{\circ}\text{C}$  freezer for 10 minutes or overnight prior to assay, then removed and allowed to air dry in a fume hood for 1-2 hours. After ethanol evaporated from the plates, 50  $\mu$ l of LANCE detection buffer (lysis buffer, 0.35% Triton X-100, 50 mM HEPES and 10 mM calcium chloride in ddH<sub>2</sub>O, pH 7.4) was added per well and left on a plate shaker for 10-15 minutes at room temperature. Meanwhile, a cAMP standard curve was generated using LANCE detection buffer and a serially diluted cAMP standard (50  $\mu$ M) ranging from 1  $\mu$ M to 10 pM. The serially diluted cAMP standards (5  $\mu$ l) and cell lysates (5  $\mu$ l) were transferred into 384-well opti-plates and sealed with a Sealplate<sup>®</sup>-A-384-well microplate adhesive film and briefly centrifuged (10 seconds, 500 rpm,  $23^{\circ}\text{C}$ ). A 1:200 dilution of LANCE assay Alexa Fluor<sup>®</sup> 647 anti-cAMP antibody was prepared in detection buffer and 5  $\mu$ l added to each well. Plates were sealed and briefly centrifuged again (10 seconds, 500 rpm,  $23^{\circ}\text{C}$ ) and left to incubate, sealed for 30 minutes at room temperature. During this incubation, detection mix was made up consisting of detection buffer, Europium-W8044 labelled streptavidin (1:4500) and biotin-cAMP (1:1500). After 30 minutes incubation, 10  $\mu$ l of detection mix was added to each well, plates were centrifuged (30 seconds, 500 rpm,  $23^{\circ}\text{C}$ ), sealed and left to incubate for 1 hour at room temperature. Plates were read after an overnight incubation on an Envision plate reader. A standard curve was included in each experiment to ensure accurate quantification of cAMP.

**Data analysis for receptor assays** Data are derived from at least three independent experiments for statistical analysis and all experiments were performed with two or three technical replicates. Quantification of cAMP was obtained from a standard curve included in each experiment and plotted using the software GraphPad Prism 6.0 (GraphPad Software Inc, San Diego, CA, USA)

with a non-linear regression 3-parameter logistic equation with a Hill slope of 1 to determine the pEC<sub>50</sub>. The pEC<sub>50</sub> values from the fits were combined from different experimental days and statistically tested for difference from the WT peptide using the Student's t-test with statistical significance defined as \* p < 0.05, \*\* p < 0.01, \*\*\* p < 0.001. Due to variability in amount of cAMP produced between experimental days, data were normalized to the control peptide for each experiment to obtain E<sub>max</sub> values. For each analogue, data were normalized to the maximum (E<sub>max</sub>) and minimum (E<sub>min</sub>) responses of h-amylin. Normalized data for each experiment were combined and statistically tested for differences between analogs and the control h-amylin peptide by an unpaired Students t-test with statistical significance defined as \* p < 0.05, \*\* p < 0.01, \*\*\* p < 0.001.

## **ASSOCIATED CONTENT**

### **Supporting Information**

This material is available free of charge via the internet at <http://pubs.acs.org> at DOI:

Sequence of amylin from different species (Figure S1), comparison of amyloidogenicity of human amylin and bovine amylin deduced by different amyloid prediction programs (Table S1), thioflavin-T kinetics assay of bovine amylin in PBS buffer (Figure S2),  $\beta$ -cell toxicity assays at different concentrations (Figure S3), Comparison of T<sub>50</sub> values for variants of human amylin corresponding to single substitutions from bovine amylin (Figure S4).

## **AUTHOR INFORMATION**

### **Corresponding Author**

\*E-mail: [daniel.raleigh@stonybrook.edu](mailto:daniel.raleigh@stonybrook.edu), Phone: (631) 632-9547; Fax: (631) 632-7960.

## **ORCID**

Daniel P. Raleigh: 0000-0003-3248-7493

## **Funding**

This work was supported by grants from the United States Public Health National Institutes of Health, GM078114, to D. P. R. and from the Marsden Fund, Royal Society of New Zealand to D.L.H.

## **Notes**

The authors declare no competing financial interest.

## **ACKNOWLEDGEMENTS**

We thank members of the Raleigh and Hay groups for helpful discussions. We thank Mr. Zachary Ridgway for providing the S29P h-amylin peptide and experimental data collected with this peptide.

## **REFERENCES:**

- (1) Montane, J., Klimek-Abercrombie, A., Potter, K. J., Westwell-Roper, C., and Bruce Verchere, C. (2012) Metabolic stress, IAPP and islet amyloid, *Diabetes Obes. Metab.* 14 Suppl 3, 68-77.
- (2) Cao, P., Marek, P., Noor, H., Patsalo, V., Tu, L. H., Wang, H., Abedini, A., and Raleigh, D. P. (2013) Islet amyloid: from fundamental biophysics to mechanisms of cytotoxicity, *FEBS Lett.* 587, 1106-1118.
- (3) Westermark, G. T., Westermark, P., Berne, C., Korsgren, O., and Transpla, N. N. C. I. (2008) Widespread amyloid deposition in transplanted human pancreatic islets, *N. Engl. J. Med.* 359, 977-979.

- (4) Potter, K. J., Abedini, A., Marek, P., Klimek, A. M., Butterworth, S., Driscoll, M., Baker, R., Nilsson, M. R., Warnock, G. L., Oberholzer, J., Bertera, S., Trucco, M., Korbitt, G. S., Fraser, P. E., Raleigh, D. P., and Verchere, C. B. (2010) Islet amyloid deposition limits the viability of human islet grafts but not porcine islet grafts, *Proc. Natl. Acad. Sci. U. S. A.* *107*, 4305-4310.
- (5) Akter, R., Cao, P., Noor, H., Ridgway, Z., Tu, L. H., Wang, H., Wong, A. G., Zhang, X., Abedini, A., Schmidt, A. M., and Raleigh, D. P. (2016) Islet amyloid polypeptide: structure, function, and pathophysiology, *J. Diabetes Res.* *2016*, 2798269.
- (6) Bower, R. L., and Hay, D. L. (2016) Amylin structure-function relationships and receptor pharmacology: implications for amylin mimetic drug development, *Br. J. Pharmacol.* *173*, 1883-1898.
- (7) Hay, D. L., Chen, S., Lutz, T. A., Parkes, D. G., and Roth, J. D. (2015) Amylin: pharmacology, physiology, and clinical potential, *Pharmacol. Rev.* *67*, 564-600.
- (8) Fineman, M. S., Koda, J. E., Shen, L. Z., Strobel, S. A., Maggs, D. G., Weyer, C., and Kolterman, O. G. (2002) The human amylin analog, pramlintide, corrects postprandial hyperglucagonemia in patients with type-I diabetes, *Metabolism* *51*, 636-641.
- (9) Gingell, J. J., Burns, E. R., and Hay, D. L. (2014) Activity of pramlintide, rat and human amylin but not A beta(1-42) at human amylin receptors, *Endocrinology* *155*, 21-26.
- (10) Westermark, P., Andersson, A., and Westermark, G. T. (2011) Islet amyloid polypeptide, islet amyloid, and diabetes mellitus, *Physiol. Rev.* *91*, 795-826.
- (11) Westermark, P., Engstrom, U., Johnson, K. H., Westermark, G. T., and Betsholtz, C. (1990) Islet amyloid polypeptide-pinpointing amino-acid-residues linked to amyloid fibril formation, *Proc. Natl. Acad. Sci. U. S. A.* *87*, 5036-5040.

- (12) Green, J., Goldsbury, C., Mini, T., Sunderji, S., Frey, P., Kistler, J., Cooper, G., and Aebi, U. (2003) Full-length rat amylin forms fibrils following substitution of single residues from human amylin, *J. Mol. Biol.* 326, 1147-1156.
- (13) Abedini, A., and Raleigh, D. P. (2006) Destabilization of human IAPP amyloid fibrils by proline mutations outside of the putative amyloidogenic domain: is there a critical amyloidogenic domain in human IAPP?, *J. Mol. Biol.* 355, 274-281.
- (14) Koo, B. W., Hebda, J. A., and Miranker, A. D. (2008) Amide inequivalence in the fibrillar assembly of islet amyloid polypeptide, *Protein Eng. Des. Sel.* 21, 147-154.
- (15) Tu, L. H., and Raleigh, D. P. (2013) Role of aromatic interactions in amyloid formation by islet amyloid polypeptide, *Biochemistry* 52, 333-342.
- (16) Deepa, P. M., Dimri, U., Jhambh, R., Yattoo, M. I., and Sharma, B. (2015) Alteration in clinico-biochemical profile and oxidative stress indices associated with hyperglycaemia with special reference to diabetes in cattle-a pilot study, *Trop. Anim. Health. Pro.* 47, 103-109.
- (17) Clark, Z. (2003) Diabetes mellitus in a 6-month-old Charolais heifer calf, *Can. Vet. J.* 44, 921-922.
- (18) Tajima, M., Yuasa, M., Kawanabe, M., Taniyama, H., Yamato, O., and Maede, Y. (1999) Possible causes of diabetes mellitus in cattle infected with bovine viral diarrhoea virus, *J. Vet. Med. B.* 46, 207-215.
- (19) Ahmed, A. B., and Kajava, A. V. (2013) Breaking the amyloidogenicity code: methods to predict amyloids from amino acid sequence, *FEBS Lett.* 587, 1089-1095.
- (20) Wong, A. G., Wu, C., Hannaberry, E., Watson, M. D., Shea, J. E., and Raleigh, D. P. (2016) Analysis of the amyloidogenic potential of pufferfish (*Takifugu rubripes*) islet amyloid

polypeptide highlights the limitations of thioflavin-T assays and the difficulties in defining amyloidogenicity, *Biochemistry* 55, 510-518.

(21) LeVine, H. (1999) Quantification of beta-sheet amyloid fibril structures with thioflavin-T, *Methods Enzymol.* 309, 274-284.

(22) Meng, F., Marek, P., Potter, K. J., Verchere, C. B., and Raleigh, D. P. (2008) Rifampicin does not prevent amyloid fibril formation by human islet amyloid polypeptide but does inhibit fibril thioflavin-T interactions: implications for mechanistic studies of beta-cell death, *Biochemistry* 47, 6016-6024.

(23) Hudson, S. A., Ecroyd, H., Kee, T. W., and Carver, J. A. (2009) The thioflavin-T fluorescence assay for amyloid fibril detection can be biased by the presence of exogenous compounds, *FEBS J.* 276, 5960-5972.

(24) Marek, P. J., Patsalo, V., Green, D. F., and Raleigh, D. P. (2012) Ionic strength effects on amyloid formation by amylin are a complicated interplay among debye screening, ion selectivity, and hofmeister effects, *Biochemistry* 51, 8478-8490.

(25) Hay, D. L., Christopoulos, G., Christopoulos, A., Poyner, D. R., and Sexton, P. M. (2005) Pharmacological discrimination of calcitonin receptor: receptor activity-modifying protein complexes, *Mol. Pharmacol.* 67, 1655-1665.

(26) Wiltzius, J. J. W., Sievers, S. A., Sawaya, M. R., Cascio, D., Popov, D., Riek, C., and Eisenberg, D. (2008) Atomic structure of the cross-beta spine of islet amyloid polypeptide (amylin), *Protein Sci.* 17, 1467-1474.

(27) Luca, S., Yau, W. M., Leapman, R., and Tycko, R. (2007) Peptide conformation and supramolecular organization in amylin fibrils: constraints from solid-state NMR, *Biochemistry* 46, 13505-13522.

- (28) Abedini, A., and Raleigh, D. P. (2009) A critical assessment of the role of helical intermediates in amyloid formation by natively unfolded proteins and polypeptides, *Protein Eng. Des. Sel.* 22, 453-459.
- (29) Wiltzius, J. J. W., Sievers, S. A., Sawaya, M. R., and Eisenberg, D. (2009) Atomic structures of IAPP (amylin) fusions suggest a mechanism for fibrillation and the role of insulin in the process, *Protein Sci.* 18, 1521-1530.
- (30) Gilead, S., Wolfenson, H., and Gazit, E. (2006) Molecular mapping of the recognition interface between the islet amyloid polypeptide and insulin, *Angew. Chem. Int. Edit.* 45, 6476-6480.
- (31) Andreetto, E., Yan, L. M., Tatarek-Nossol, M., Velkova, A., Frank, R., and Kapurniotu, A. (2010) Identification of hot regions of the A beta-IAPP interaction interface as high-affinity binding sites in both cross- and self-association, *Angew. Chem. Int. Edit.* 49, 3081-3085.
- (32) Cao, P., Tu, L. H., Abedini, A., Levsh, O., Akter, R., Patsalo, V., Schmidt, A. M., and Raleigh, D. P. (2012) Sensitivity of amyloid formation by human islet amyloid polypeptide to mutations at residue 20, *J. Mol. Biol.* 421, 282-295.
- (33) Jha, S., Snell, J. M., Sheftic, S. R., Patil, S. M., Daniels, S. B., Kolling, F. W., and Alexandrescu, A. T. (2014) pH dependence of amylin fibrillization, *Biochemistry* 53, 300-310.
- (34) Kikumoto, K., Katafuchi, T., and Minamino, N. (2003) Specificity of porcine calcitonin receptor and calcitonin receptor-like receptor in the presence of receptor-activity-modifying proteins, *Hypertens. Res.* 26 Suppl, S15-23.
- (35) Bailey, R. J., Walker, C. S., Ferner, A. H., Loomes, K. M., Prijic, G., Halim, A., Whiting, L., Phillips, A. R., and Hay, D. L. (2012) Pharmacological characterization of rat amylin

receptors: implications for the identification of amylin receptor subtypes, *Br. J. Pharmacol.* *166*, 151-167.

(36) Johansson, E., Hansen, J. L., Hansen, A. M. K., Shaw, A. C., Becker, P., Schaffer, L., and Reedtz-Runge, S. (2016) Type II turn of receptor-bound salmon calcitonin revealed by X-ray crystallography, *J. Biol. Chem.* *291*, 13689-13698.

(37) Booe, J. M., Walker, C. S., Barwell, J., Kuteyi, G., Simms, J., Jamaluddin, M. A., Warner, M. L., Bill, R. M., Harris, P. W., Brimble, M. A., Poyner, D. R., Hay, D. L., and Pioszak, A. A. (2015) Structural basis for receptor activity-modifying protein-dependent selective peptide recognition by a G protein-coupled receptor, *Mol. Cell* *58*, 1040-1052.

(38) Lee, S. M., Hay, D. L., and Pioszak, A. A. (2016) Calcitonin and amylin receptor peptide interaction mechanisms. Insights into peptide-binding modes and allosteric modulation of the calcitonin receptor by receptor activity-modifying proteins, *J. Biol. Chem.* *291*, 8686-8700.

(39) Gingell, J. J., Simms, J., Barwell, J., Poyner, D. R., Watkins, H. A., Pioszak, A. A., Sexton, P. M., and Hay, D. L. (2016) An allosteric role for receptor activity-modifying proteins in defining GPCR pharmacology, *Cell Discov* *2*, 16012.

(40) Kowalczyk, R., Brimble, M. A., Tomabechi, Y., Fairbanks, A. J., Fletcher, M., and Hay, D. L. (2014) Convergent chemoenzymatic synthesis of a library of glycosylated analogues of pramlintide: structure-activity relationships for amylin receptor agonism, *Org. Biomol. Chem.* *12*, 8142-8151.

(41) Dunkelberger, E. B., Buchanan, L. E., Marek, P., Cao, P., Raleigh, D. P., and Zanni, M. T. (2012) Deamidation accelerates amyloid formation and alters amylin fiber structure, *J. Am. Chem. Soc.* *134*, 12658-12667.

- (42) Bischoff, R., and Kolbe, H. V. J. (1994) Deamidation of asparagine and glutamine residues in proteins and peptides - structural determinants and analytical methodology, *J. Chromatogr. B.* 662, 261-278.
- (43) Wakankar, A. A., and Borchardt, R. T. (2006) Formulation considerations for proteins susceptible to asparagine deamidation and aspartate isomerization, *J. Pharm. Sci.* 95, 2321-2336.
- (44) Wang, H., Abedini, A., Ruzsicska, B., and Raleigh, D. P. (2014) Rationally designed, nontoxic, nonamyloidogenic analogues of human islet amyloid polypeptide with improved solubility, *Biochemistry* 53, 5876-5884.
- (45) Abedini, A., Plesner, A., Cao, P., Ridgway, Z., Zhang, J., Tu, L. H., Middleton, C. T., Chao, B., Sartori, D. J., Meng, F., Wang, H., Wong, A. G., Zanni, M. T., Verchere, C. B., Raleigh, D. P., and Schmidt, A. M. (2016) Time-resolved studies define the nature of toxic IAPP intermediates, providing insight for anti-amyloidosis therapeutics, *Elife* 5, 10.7554/eLife.12977.
- (46) Bailey, R. J., and Hay, D. L. (2006) Pharmacology of the human CGRP1 receptor in Cos 7 cells, *Peptides* 27, 1367-1375.
- (47) Gingell, J. J., Qi, T., Bailey, R. J., and Hay, D. L. (2010) A key role for tryptophan 84 in receptor activity-modifying protein 1 in the amylin 1 receptor, *Peptides* 31, 1400-1404.

## FIGURE LEGENDS

**Figure 1:** (a) Primary sequence of human and bovine amylin. The polypeptides have an amidated C-terminus and an intramolecular disulfide bond between residue 2 and 7. Residues in bovine amylin which differ from those in human amylin are colored blue. (b) A top down view of a model of the human amylin amyloid fibril based on crystal structures of small fragments of h-amylin.<sup>26</sup> Residues in bovine amylin that differ from human amylin are shown in space filling format together with some of the key residues that they interact with. (c) A side view of the structure in ribbon format. The N-terminal  $\beta$ -strand in each monomer is colored blue, the C-terminal  $\beta$ -strand red, while the disordered region and the loop which connects the two  $\beta$ -strands are colored green.

**Figure 2:** Bovine amylin does not form amyloid in Tris buffer. (a) Thioflavin-T fluorescence experiments comparing the kinetics of amyloid formation by human amylin (black) and bovine amylin (blue). (b) TEM images were recorded at different time points. No amyloid formation was observed for bovine amylin for up to 21 days. Experiments were conducted using 16  $\mu$ M peptide, 32  $\mu$ M thioflavin-T at pH 7.4, 25°C and in 20 mM Tris. Scale bar represents 100 nm.

**Figure 3:** Bovine amylin is not toxic to cultured rat INS-1  $\beta$ -cells. The results of 24 hours incubation of bovine and human amylin are displayed. Human amylin (black) and bovine amylin (blue) were incubated on rat INS-1  $\beta$ -cells for 24 hours and cell viability assessed using Alamar Blue assays. Final peptide concentrations were 15 $\mu$ M, 22  $\mu$ M and 30 $\mu$ M. Data are normalized to cells treated with media (gray). Error bars represent the standard deviation of 3 independent measurements.

**Figure 4:** Bovine amylin exhibits reduced potency at human amylin receptors. Concentration-response curves of cAMP production by h-amylin compared with b-amylin at (a) hCT<sub>(a)</sub>, and (b) hAMY<sub>1(a)</sub> receptors expressed in Cos-7 cells. Curves are plotted as a percentage of maximal h-

amylin stimulated cAMP production and data points are the mean  $\pm$  SEM from 3 independent experiments.

**Figure 5:** Mutational analysis of amyloid formation by human amylin reveals the importance of non-conservative substitutions in modulating amyloidogenicity. Thioflavin-T fluorescence experiments comparing the kinetics of amyloid formation by wildtype h-amylin (black) and (a) H18P h-amylin (red); (b) N22K h-amylin (green); (c) S29P h-amylin (purple) and (d) N31K h-amylin (brown). Data normalized relative to their final maximum fluorescence intensity. TEM images were collected at the end of the kinetics experiment. Experiments were conducted using 16  $\mu$ M peptide, 32  $\mu$ M thioflavin-T at pH 7.4, 25°C and in 20 mM Tris. Scale bars represent 100 nm.

**Figure 6:** Mutational analysis of the reduced  $\beta$ -cell toxicity by bovine amylin. The effects of incubating H18P h-amylin (red), N22K h-amylin (green), S29P h-amylin (purple), human amylin (black), and bovine amylin (blue) on rat INS-1  $\beta$ -cells at 30  $\mu$ M concentration for 24 hours and 48 hours. Cell viability measured using Alamar Blue assays. Data are normalized relative to cells treated with media (gray).

**Figure 7:** Concentration-response curves of cAMP production by h-amylin compared with h-amylin analogs with single-residue substitutionss from the b-amylin sequence at the hAMY<sub>1(a)</sub> receptor expressed in Cos-7 cells. Curves are plotted as a percentage of maximal h-amylin stimulated cAMP production and data points represent the mean  $\pm$  SEM from 3-6 independent experiments.

Figure 1:

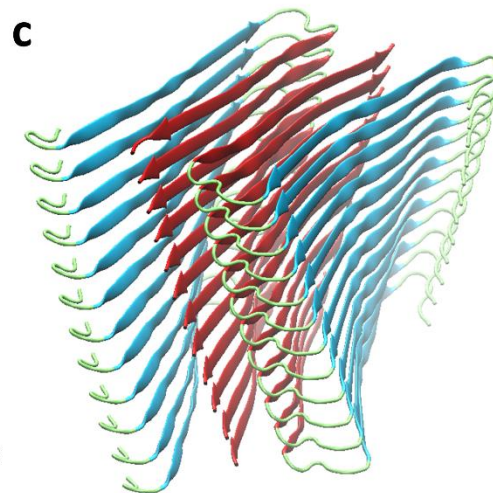
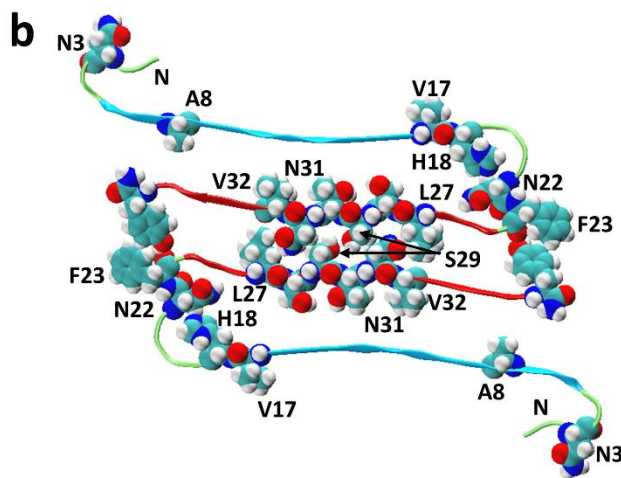


Figure 2:

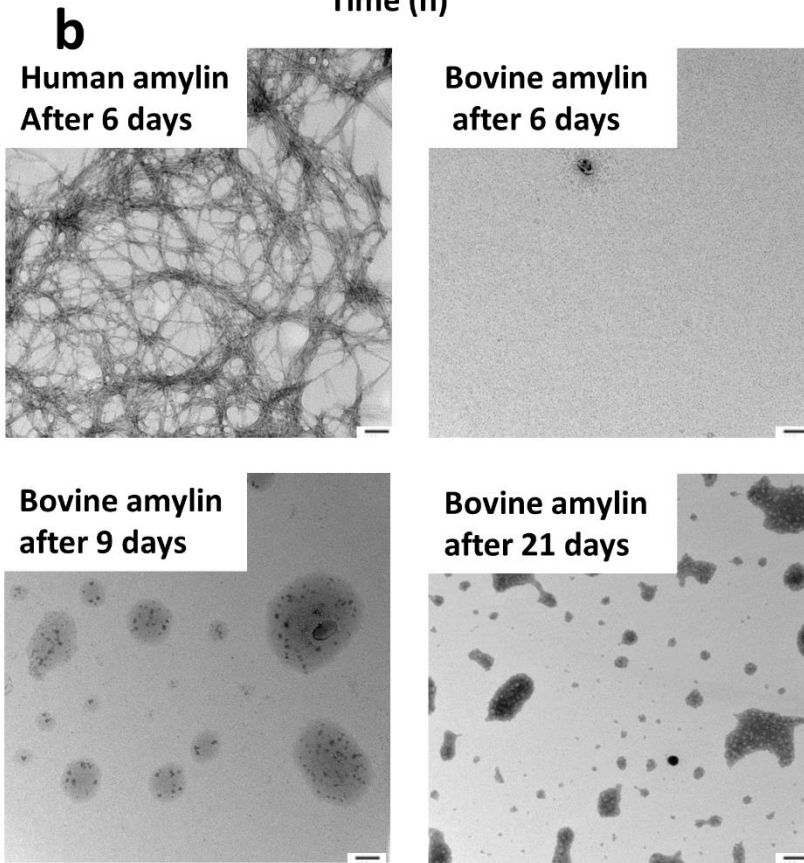
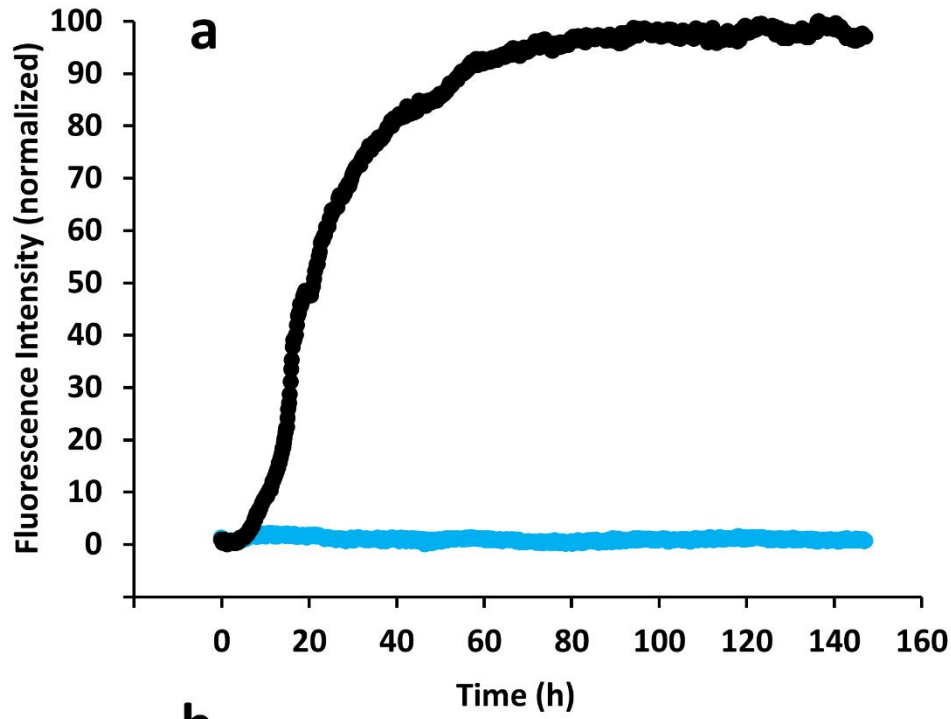


Figure 3:

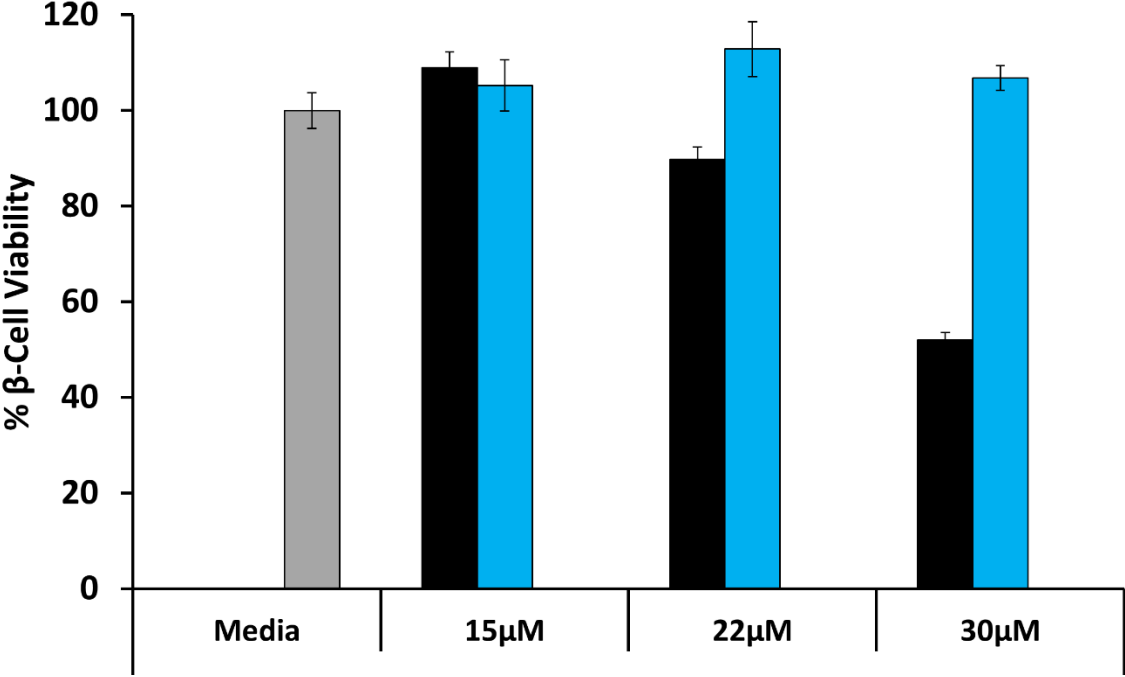


Figure 4:

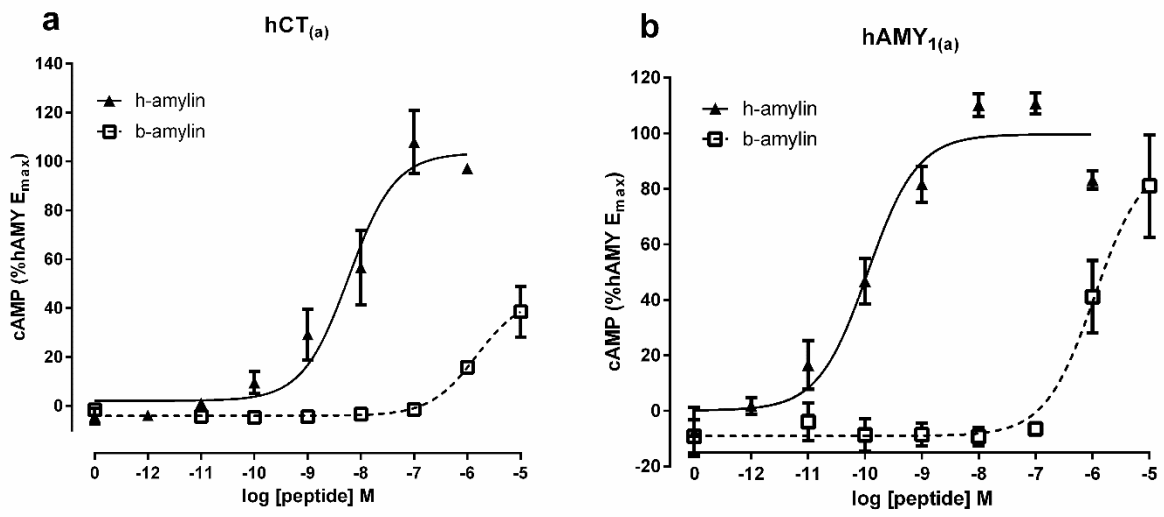


Figure 5:

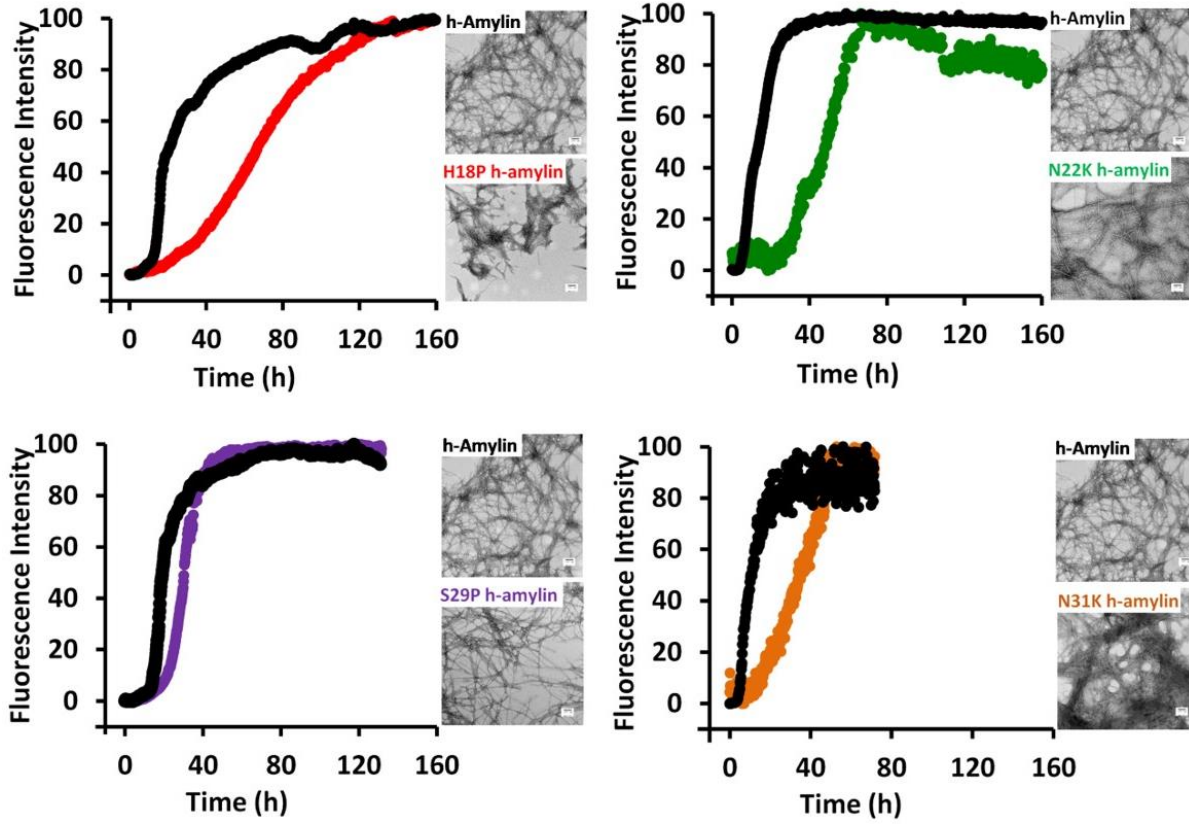


Figure 6:

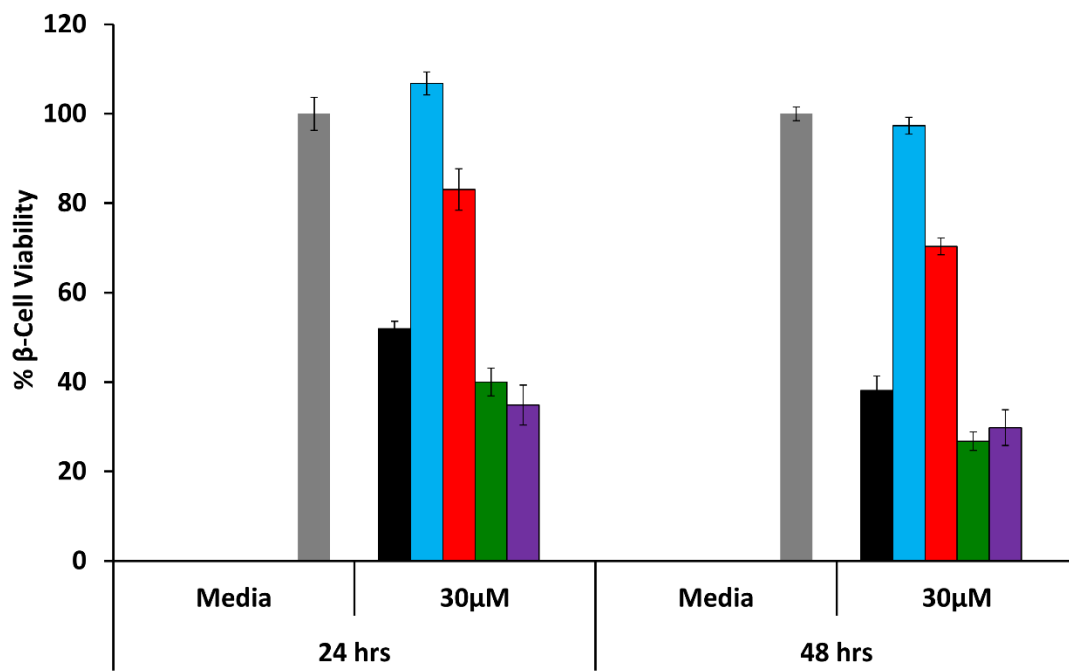
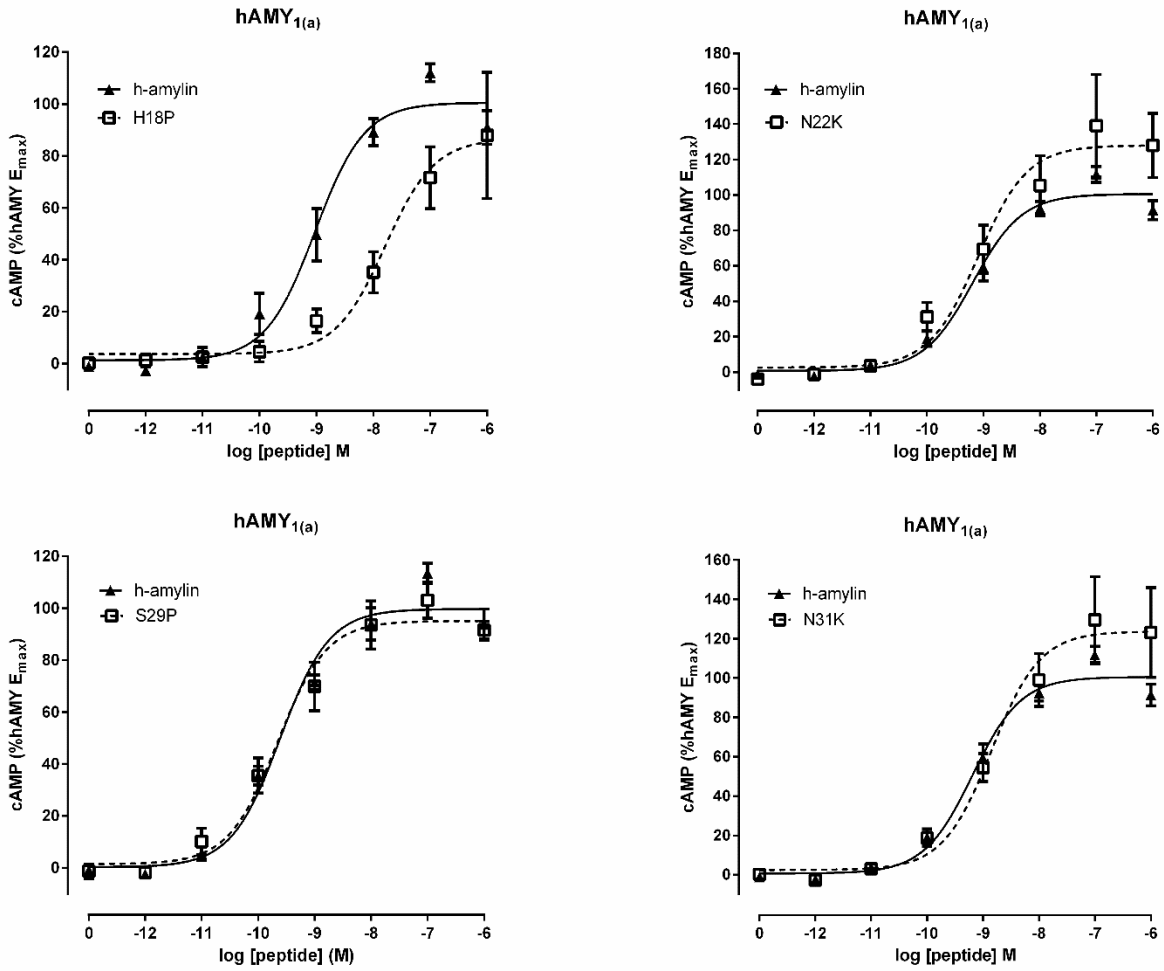


Figure 7:



**Table 1:** Summary of activity data for wild type h-amylin, b-amylin and the four single residue analogs including pEC<sub>50</sub> and E<sub>max</sub> values at the hCT<sub>(a)</sub> and hAMY<sub>1(a)</sub> receptors. \* p < 0.05, \*\* p < 0.01, \*\*\* p < 0.001 by unpaired t-test compared to h-amylin.

	pEC <sub>50</sub>						E <sub>max</sub>	
	hCT <sub>(a)</sub>	Fold-change	n	hAMY <sub>1(a)</sub>	Fold-change	n	hCT <sub>(a)</sub>	hAMY <sub>1(a)</sub>
h-amylin	8.38 ± 0.34	-338	3	9.94 ± 0.22	> -1000	3	100	
b-amylin	5.85 ± 0.22**			5.95 ± 0.15***			41.1 ± 12.2**	93.8 ± 22.7
h-amylin	8.43 ± 0.16	- 6.6	3	9.10 ± 0.23	-20	3	100	
H18P	7.61 ± 0.09*			7.79 ± 0.10**			79.8 ± 10.3	87.7 ± 21.2
h-amylin	8.89 ± 0.20	-1.3	6	9.21 ± 0.13	-1.8	6	100	
N22K	8.84 ± 0.20			8.96 ± 0.18			136 ± 25.6	131 ± 21.1
h-amylin	8.78 ± 0.07	-1.5	4	9.67 ± 0.11	-1.2	3	100	
S29P	8.60 ± 0.25			9.59 ± 0.19			83.1 ± 6.88	94.4 ± 5.52
h-amylin	8.89 ± 0.29	-1.8	6	9.21 ± 0.13	-2.3	6	100	
N31K	8.63 ± 0.22			8.85 ± 0.17			160 ± 39.0	126 ± 21.4

## Table of Contents Graphic

